# Dynamic targeting of microtubules by TPPP/p25 affects cell survival

**Atilla Lehotzky[1,*], László Tirián[2,*], Natália Tökési[1], Péter Lénárt[3], Bálint Szabó[4], János Kovács[5] and Judit Ovádi[1,‡]**

[1]Institute of Enzymology, Biological Research Center, Hungarian Academy of Sciences, 1113 Budapest, Hungary
[2]Department of Biology, Faculty of Medicine, University of Szeged, 6720 Szeged, Hungary
[3]European Molecular Biology Laboratory, 69117 Heidelberg, Germany
[4]Biological Physics Research Group, Hungarian Academy of Sciences, 1117 Budapest, Hungary
[5]Department of General Zoology, Eötvös University of Sciences, 1117 Budapest, Hungary
*These authors contributed equally to this work
‡Author for correspondence (e-mail: ovadi@enzim.hu)

*Accepted 21 September 2004*
*Journal of Cell Science 117, 6249-6259 Published by The Company of Biologists 2004*
*doi:10.1242/jcs.01550*

## Summary

**Recently we identified TPPP/p25 (tubulin polymerization promoting protein/p25) as a brain-specific unstructured protein that induced aberrant microtubule assemblies and ultrastructure in vitro and as a new marker for Parkinson's disease and other synucleopathies. In this paper the structural and functional consequences of TPPP/p25 are characterized to elucidate the relationship between the in vitro and the pathological phenomena. We show that at low expression levels EGFP-TPPP/p25 specifically colocalizes with the microtubule network of HeLa and NRK cells. We found that the colocalization was dynamic ($t_{½}$=5 seconds by fluorescence recovery after photobleaching) and changed during the phases of mitosis. Time-lapse and immunofluorescence experiments revealed that high levels of EGFP-TPPP/p25 inhibited cell division and promoted cell death. At high expression levels or in the presence of proteosome inhibitor, green fusion protein accumulated around centrosomes forming an aggresome-like structure protruding into the nucleus or a filamentous cage of microtubules surrounding the nucleus. These structures showed high resistance to vinblastin. We propose that a potential function of TPPP/p25 is the stabilization of physiological microtubular ultrastructures, however, its upregulation may directly or indirectly initiate the formation of aberrant protein aggregates such as pathological inclusions.**

Supplementary material available online at
http://jcs.biologists.org/cgi/content/full/117/25/6249/DC1

Key words: Aggresome, Cytoskeleton, EGFP, Microtubules, Neurodegeneration

## Introduction

Most cellular proteins are folded into a defined conformation that comprises their function, however there is a recently discovered family of natively unfolded proteins denoted as intrinsically unstructured proteins (Uversky, 2002a). It has been established that deposition of unfolded proteins is related to several neurodegenerative disorders (reviewed by Uversky, 2002b). The formation of inclusions has been detected and analyzed at the cellular level and these data indicate that various unstructured proteins, including α-synuclein, parkin and misfolded membrane proteins, can induce the formation of aggresome-like structures in response to excess levels of unwanted protein (Johnston et al., 1998; Garcia-Mata et al., 1999; Junn et al., 2002; Tanaka et al., 2004).

Tubulin polymerization-promoting protein (TPPP/p25) was independently identified as a brain-specific protein occurring mainly in oligodendrocytes and in the neuropil (Takahashi et al., 1993) and as a basic, heat-stable tubulin-binding protein that at substoichiometric concentration promotes the polymerization of tubulin into double-walled tubules, polymorphic aggregates and bundles of paclitaxel-stabilized microtubules in vitro (Hlavanda et al., 2002). The sequence of this protein differs from that of other proteins identified so far, however, it shows high homology with TPPP/p25-like hypothetical proteins identified using BLAST database searches (Tirian et al., 2003; Hlavanda, 2002). Our recent CD and NMR experiments provide evidence that TPPP/p25 is an intrinsically unstructured protein (Hlavanda et al., 2002; Kovács et al., 2004). Other proteins such as α-synuclein and β-amyloid involved in neurodegenerative diseases have unfolded structures (Goedert, 2001).

Recently we reported that the injection of bovine TPPP/p25 into dividing *Drosophila* embryos expressing tubulin-GFP fusion protein inhibited mitotic spindle assembly and nuclear envelope breakdown without affecting other cellular events like centrosome replication and separation, microtubule nucleation by the centrosomes and nuclear growth. We identified GTP as a specific ligand that counteracts TPPP/p25 both in vitro and in vivo (Tirian et al., 2003). Martin et al. demonstrated that p24 (corresponding to TPPP/p25) bound to the heat resistant glycogen synthase kinase 3 (GSK 3) and inhibited the kinase activity (Martin et al., 2002). By using a novel affinity technique, protein-protein interactions were identified exhibiting previously unknown memory-specific changes, and p25α (corresponding to

TPPP/p25) was found as an interacting partner of complexin, one of ten structural proteins probably involved in synaptic structural reorganization (Nelson et al., 2004).

Recently we demonstrated by immunohistochemistry and confocal microscopy that TPPP/p25 is enriched in filamentous α-synuclein bearing the Lewy bodies of Parkinson's disease and diffuse Lewy body disease, as well as glial inclusions of multiple system atrophy (Kovacs et al., 2004). In contrast, TPPP/p25 is not associated with the abnormally phosphorylated tau observed in various inclusions of Pick's disease (PiD), progressive supranuclear palsy and corticobasal degeneration. However, electron microscopy reveals clusters of TPPP/p25 immunoreactivity along filaments of the non-compact neurofibrillary tangles in Alzheimer's disease suggesting the involvement of TPPP/p25 in tau fibril formation. Unlike α-synuclein, TPPP/p25 immunoreactivity is present also in the granules of granulovacuolar degeneration in Alzheimer's disease and Pick's disease. This might reflect the sequestration process of potentially aberrant microtubular components related to TPPP/p25.

The major objective of this work was to assess the localization and the effect of TPPP/p25 on the cell architecture, specifically on the microtubular network of mammalian cells under conditions that mimic physiological and pathological states. For these purposes mammalian cells were transfected using pEGFP-TPPP/p25, and the cellular and molecular response to the expression of the fusion protein was investigated. Our data suggested that low and high expression levels of EGFP-TPPP/p25 might be related to the physiological and pathological circumstances, respectively. Although at low expression levels it colocalized with the microtubular network maintaining its physiological architecture, at higher expression levels TPPP/p25 promoted the rearrangement of microtubular network into two well-defined aberrant structures. These structures were characterized extensively using wide range of methods. In the present paper the effects of TPPP/p25 overexpression on the stability of the microtubular network and on the energy state and division of the cells are demonstrated. In addition, the formation of inclusions possibly related to neurodegenerative processes are presented.

## Materials and Methods

### DNA manipulation of TPPP/p25 coding sequence

The coding region of human TPPP/p25 (Kovacs et al., 2004) was fused to the C terminus of EGFP by cloning TPPP/p25 ORF into pEGFP-C1 (Clontech) using the *Bgl*II and *Eco*RI restriction sites producing pEGFP-TPPP/p25. To create a mammalian expression vector that enables expression of p25 without a tag, we cloned human TPPP/p25 ORF into pcDNA3 (Invitrogen) using the *Bam*HI and *Eco*RI restriction sites (pcDNA3-TPPP/p25). $His_6$-tagged human TPPP/p25 was expressed in *Escherichia coli* and purified on Talon resin (Clontech) according to the manufacturer's protocol.

### Cell culture and transfections

HeLa (ATCC, CCL-2) or normal rat kidney (NRK) cells (Daigle et al., 2001) were grown in DME/F-12 medium supplemented with 10% FCS, 1 mM sodium pyruvate, 100 U/ml streptomycin and 100 μg/ml penicillin (all from Sigma) (complete medium) in a humidified 37°C incubator with 5% $CO_2$. Cells were transfected with Fugene 6 (Roche) or ExGen 500 transfection reagent (Fermentas) according to the manufacturer's instruction and were processed about 20 hours after transfection unless indicated otherwise. For immunofluorescence and live cell studies, cells were grown on 12 mm diameter coverslips and transfected with 50 ng DNA, otherwise they were grown on 60 mm dishes. In the experiments where indicated, the transfected cells were treated 1 μM MG132 or 100 nM VBL (Sigma) in the last two hours (18-20 hours) of transfection.

### Live cell imaging

Tetramethylrhodamine ethyl ester (TMRE) uptake was used to characterize mitochondrial membrane polarization in live experiments (Iijima et al., 2003). Transfected cells were incubated with 50 nM TMRE in complete medium for 20 minutes. Cells on coverslips were washed with incubation medium (PBS supplemented with 50 nM TMRE, 1 mM sodium pyruvate and 1 g/l glucose), then the coverslips were placed on slides with cells facing up. The cells were covered in incubation medium with an extra coverslip and were sealed with molten agarose. Fluorescent images of live cells were recorded within one hour. The EGFP signal was detected with a narrow band GFP filter set (Chroma Technology). TMRE fluorescence was detected with Leica filter set N2.1 and illumination of samples was kept to a minimum. Images were recorded on a Leica DMLS microscope (Leica Microsystems, Germany) equipped with cooled CCD camera (Spot, Digital Instruments, USA), with a C-PLAN 100× immersion objective. Spot 4.0.2 was used to acquire digital images. Images were processed by Adobe Photoshop.

### Time-lapse microscopy

Time-lapse recordings were performed on a computer-controlled Leica DM IRB inverted microscope equipped with a 20× objective and an Olympus Camedia 4040z digital camera. Cell cultures were kept at 37°C in a humidified 5% $CO_2$ atmosphere within a custom-made incubator attached to the microscope stage (Hegedus et al., 2000). Phase-contrast images were acquired every 5 minutes for 2-4 days; fluorescent images were captured manually.

### FRAP analysis of TPPP/p25 dynamics on microtubule bundles

Fluorescent recovery after photobleaching (FRAP) experiments were done as described earlier (Daigle et al., 2001). Transfected NRK cells were investigated and cells expressing the construct were selected. Initially three consecutive images were taken every second with a 488 nm low intensity laser beam. The marked area containing a thick microtubule bundle was bleached three times with maximum intensity. After bleaching, recovery of fluorescence was followed at 1 second intervals with the same laser intensity as before bleaching. Fluorescent intensities upon a thick microtubule bundle in the bleached and a control area were calculated with ImageQuant 5.2 Software (Molecular Dynamics). Background fluorescence was corrected by subtracting the average fluorescent intensity of an intact area without excitation. Experiments were performed on a LSM 510 confocal microscope (Carl Zeiss, Jena, Germany).

### Immunostaining

Transfected HeLa and NRK cells were grown on coverslips. Cells were fixed either with cold methanol or with 3.7% formaldehyde in PBS for 12 minutes, or cells were fixed in cold buffered ethanol (96% ethanol:PBS, 9:1) for 12 minutes. Cells were washed in PBS and PBS containing 0.1% Triton X-100 (TPB), then were blocked for 30 minutes in TPB containing 5% FCS (TPB-FCS). Subsequently, cells were stained with monoclonal anti α-tubulin (DM1A, Sigma), monoclonal anti-vimentin (clone N9, Sigma) and anti-TPPP/p25 rat serum (Kovacs et al., 2004), in the case of pcDNA3-TPPP/p25, primary antibodies, followed by FITC-conjugated anti-rat and Texas Red-conjugated anti-mouse antibodies (Jackson Laboratories) were

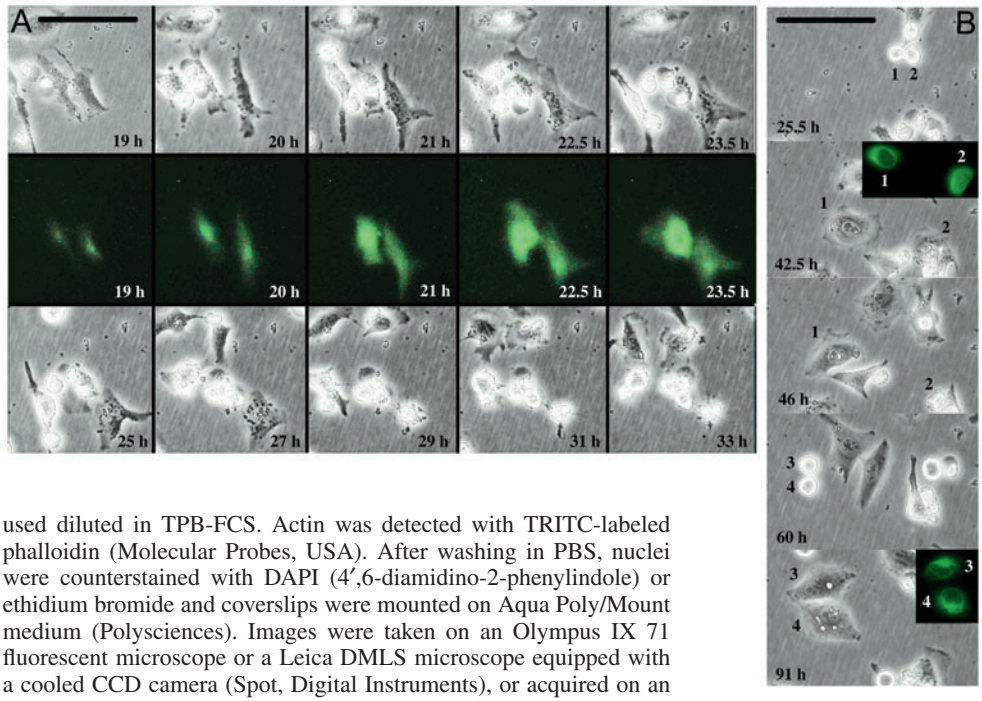


**Fig. 1.** Phase-contrast and fluorescent images of HeLa cells transfected with pEGFP-TPPP/p25 from time-lapse recordings. (A) Transfected cultures of HeLa cells were maintained and imaged on a microscope stage by phase-contrast and epifluorescence. A pair of cells is shown with increasing fluorescence over time. (B) Phase-contrast frames were selected from a time-lapse recording with fluorescent insets. Cells marked 1 and 2 did not show detectable fluorescence before division. Later, they became fluorescent, as shown in the image captured at 42.5 hours. Cell 2 died at 46 hours; cell 1 divided into cells 3 and 4 at 60 hours. Cells 3 and 4 were still alive after 91 hours. Time elapsed after transfection with pEGFP-TPPP/p25 is indicated in the lower left corners. Bar, 100 μm.

used diluted in TPB-FCS. Actin was detected with TRITC-labeled phalloidin (Molecular Probes, USA). After washing in PBS, nuclei were counterstained with DAPI (4′,6-diamidino-2-phenylindole) or ethidium bromide and coverslips were mounted on Aqua Poly/Mount medium (Polysciences). Images were taken on an Olympus IX 71 fluorescent microscope or a Leica DMLS microscope equipped with a cooled CCD camera (Spot, Digital Instruments), or acquired on an LSM 510 confocal microscope. In the case of quantitative analysis, pictures were taken with fixed exposition parameters. Analyses of digital images were made with ImageJ software (PC-based version of NIH Image). Images were processed with analySIS, Adobe Photoshop or Corel PhotoPaint software.

### Electron microscopy

HeLa cells transfected on glass coverslips were fixed for 1 hour in 0.1 M sodium cacodylate containing 1.5% paraformaldehyde, 1% glutaraldehyde, 1% sucrose and 2 mM $CaCl_2$. After washing they were post-fixed in 0.5% $OsO_4$, stained with 2% uranyl acetate, dehydrated and embedded in Durcupan (Fluka, Switzerland). In some experiments the cells were collected by trypsinization and pelleted in a microfuge before fixation. The sections were examined in a JEOL100CX electron microscope (JEOL, USA) operated at 60 kV.

### Effect of TPPP/p25 on depolymerization of taxol-treated microtubules

For turbidity measurements, absorbance was monitored at 350 nm with a Cary 100 spectrophotometer (Varian, USA). Tubulin (100 μM) was assembled to microtubules at 37°C in 50 mM Mes buffer (pH 6.6), containing 50 mM KCl, 1 mM $MgCl_2$, 1 mM EGTA (polymerization buffer) as described (Hlavanda et al., 2002). Microtubule assembly was initiated with 20 μM taxol. TPPP/p25 bundled microtubules were made by preincubating 15 μM microtubules with 3 μM TPPP/p25 at 37°C for 15 minutes in 0.1 M PIPES buffer (pH 6.6) containing 1 mM EGTA and 1 mM $MgCl_2$ (PEM buffer). Depolymerization of microtubules in control samples was carried out in the same manner (15 μM in PEM buffer). Depolymerization of samples with a final $Ca^{2+}$ concentration of 0.75 mM was induced by decreasing the temperature to 4°C and adding 5 μM vinblastin. The reactions were followed for 60 minutes.

## Results

### Time-course of expression of EGFP-TPPP/p25 in living cells

Untransfected HeLa and NRK cells do not contain endogenous TPPP/p25 in amounts detectable by immunochemistry or immunoblotting (data not shown). Thus, to examine the consequence of TPPP/p25 expression, HeLa cells were transfected with pEGFP-TPPP/p25 or empty pEGFP-C1 constructs and the time course of expression of corresponding proteins was followed in live cells by fluorescent microscopy at low magnification. The number of fluorescent cells increased with time following transfection at 20 hours. After 20 hours there was virtually no difference in the number of the EGFP-TPPP/p25-expressing cells and control EGFP-expressing cells. However, after 48 hours the number of EGFP-TPPP/p25 positive cells decreased by about 60%, indicating that long-term expression of EGFP-TPPP/p25 leads to cell death with dramatic morphological changes and no movement of the cells (data not shown).

To follow the fate of individual cells we performed time-lapse experiments on HeLa cells after their transfection with EGFP-TPPP/p25 and overnight incubation. Phase-contrast images were collected automatically every 5 minutes and transformed into movies, fluorescent images were captured manually 15 times a day. In this way we could identify and follow the transfected cells in the phase-contrast movies. In three sets of experiments we tracked 55 transfected cells for 30 hours, in the ~20-50 hour interval after transfection. In living cells the intensity of fluorescence increased as a function of time (Fig. 1A), which led to the death of most (33) cells according to the observed morphological changes. Virtually no division of the fluorescent cells was observed in the above interval. After this period we observed mitosis of cells with low fluorescent intensity in few cases (Fig. 1B). Interestingly, labeled cells were found in pairs close to each other, and phase-contrast movies showed that these pairs are sister cells (Fig. 1B, first two frames). During the period of observation all 24 newly appearing cells were found to be the offspring (12 pairs of sister cells) of a previously dividing, apparently unlabeled cell.

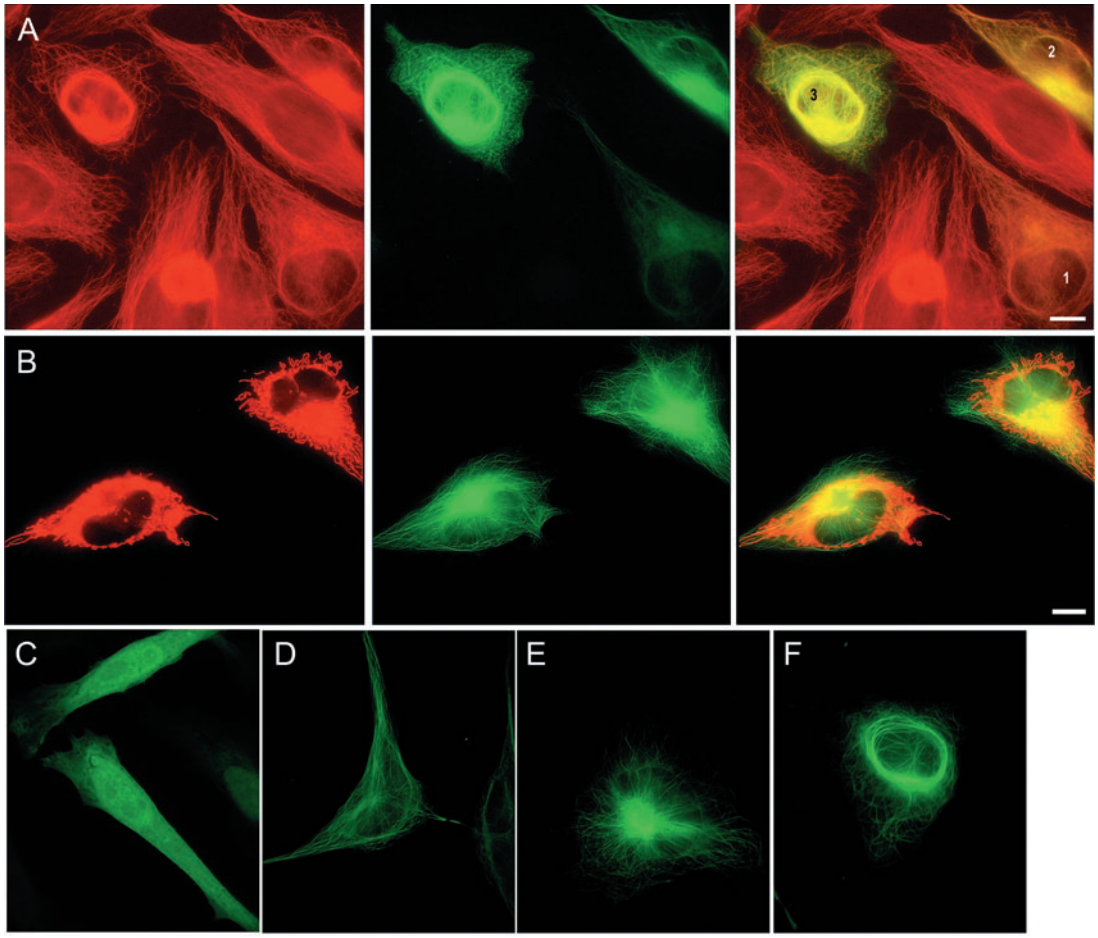


**Fig. 2.** Overview of HeLa cells transfected with pEGFP-TPPP/p25. (A) Cells were fixed in cold-buffered ethanol for immunocytochemistry with anti-tubulin antibody. The representative image shows three TPPP/p25-transfected cells with distinct morphologies in the same microscopic field. Note the colocalization (orange) of EGFP-TPPP/p25 (green) with the microtubular network (red) at low expression levels (cell marked 1). The other two cells with bright fluorescence show an aberrant microtubular network and morphological changes with colocalization (marked 2 and 3). Comparing the fluorescence of these three transfected cells suggests low (cell 1) and high (cells 2 and 3) levels of expressed protein. (B) TMRE uptake in transfected HeLa cells. TMRE (red) was used to investigate mitochondrial membrane state in live cells. At low levels of expression, the cells show a polarization state similar to that of untransfected cells. (C) HeLa cells transfected with pEGFP-C1 plasmid. Note the strong nuclear presence of the EGFP protein. (D-F) HeLa cells transfected with EGFP-TPPP/p25 plasmid. Representative examples of the different expression 'classes' are presented: (D) low-level expressing; (E) aggresome-like; (F) nuclear cage. Bars, 10 μm.

### Distinct cellular structures in pEGFP-TPPP/p25 transfected mammalian cells

Anti-α-tubulin antibody was used to gain an overall view of the pEGFP-TPPP/p25 transiently transfected HeLa cells by immunocytochemistry (Fig. 2A). Three transfected cells with different green and orange fluorescent intensities are shown: the cell labeled 1 shows a low amount of EGFP-TPPP/p25 expression; the organization of microtubular network is similar to that of non-transfected controls (red only); this we denoted a 'low expression state'. In other cells, labeled 2 and 3, heavy accumulation of the fusion protein on microtubules and in proximity to the microtubule organization center was observed. The morphology as well as the architecture of the microtubular network was altered in these cells when compared to the non-transfected controls. This type of staining we denoted 'high expression state'. Distinct morphology and the cytoskeleton network decorated with green fluorescent TPPP/p25 can be also visualized in transfected HeLa cells depending upon the expression level of the fusion protein (Fig. 2D-F). When cells were transfected with pEGFP-C1 plasmid, the fluorescent signal was homogeneously distributed in the cytoplasm and also accumulated in the nucleus (Fig. 2C).

Mitochondrial membrane potential that regulates the production of high-energy phosphate is an important parameter determining the fate of the cells (Iijima et al., 2003). Therefore, a fluorescent dye, TMRE, which forms hyperpolarized membranes upon its extensive accumulation (Collins and Bootman, 2003), was used to study the membrane-related energy-producing system at low and high expression states in EGFP-TPPP/p25 transfected cells. Cells expressing EGFP-TPPP/p25 at low levels displayed a TMRE signal (red) similar to the control cells (Fig. 2B). In addition, comparison of the distribution of red and green fluorescence indicated that the fusion protein does not bind to intact mitochondria. However, in transfected cells with high EGFP fluorescence intensity and altered morphology, the red fluorescence is virtually

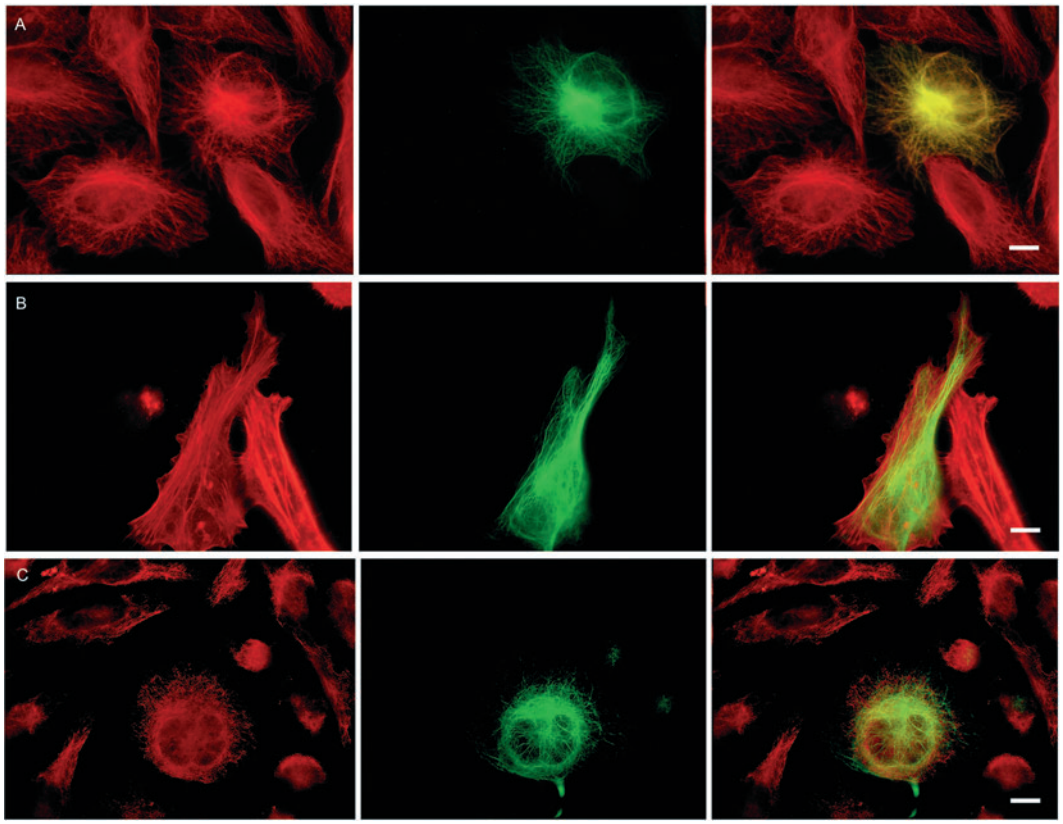


**Fig. 3.** HeLa cells transfected with pEGFP-TPPP/p25 and their filamentous networks. (A-C) Cells were transfected and incubated for 20 hours, fixed with cold ethanol for immunocytochemistry to detect the alignment of TPPP/p25 (green) with tubulin (A), actin (B) and vimentin (C) (all red). (A) The microtubular network is not affected in the transfected cell, however, accumulation of fluorescent material started at the perinuclear position. Virtually complete colocalization with microtubules is observed. (B) Actin filaments show complete dislocation with the green EGFP-TPPP/p25 signal. Red and green images were taken at different positions on the *z*-axis to get focused signals. (C) Intermediate filaments (vimentin) do not show colocalization with EGFP-TPPP/p25. Bars, 10 μm.

undetectable (data not shown). The loss of red signal indicates the collapse of the mitochondrial membrane potential because of mitochondrial dysfunction.

### Specific colocalization of TPPP/p25 with the microtubular network

In order to test the specificity of colocalization of TPPP/p25 and the microtubular network, the different filaments of HeLa cells transfected with pEGFP-TPPP/p25 were investigated. Although an excellent alignment of the fluorescent fusion protein with the microtubular network was observed (Fig. 3A), EGFP-TPPP/p25 did not align along the actin filaments and colocalization of the green protein with the actin filaments detected by phalloidin binding (red) could not be visualized by fluorescence microscopy (Fig. 3B). In addition, disruption of the actin network by treatment with cytochalasin did not change its subcellular distribution (data not shown). One of the intermediate filament groups was visualized by using a monoclonal vimentin antibody. The green fusion protein did not appear to colocalize with the filamentous structure of vimentin (Fig. 3C), however, some rearrangement of this filament system cannot be excluded (see below).

### The distribution of EGFP-TPPP/p25 during the cell cycle

The localization of EGFP-TPPP/p25 was studied at different stages of the cell cycle by immunocytochemistry in NRK cells expressing the EGFP fusion protein at low levels. For visualization of the microtubular network and nucleus, the cells were stained with anti-α-tubulin and DAPI, respectively. EGFP localized along the microtubule network in interphase cells (Fig. 4). TPPP/p25 is enriched at the region of the microtubule-organizing centers whereas less TPPP/p25 is present on the microtubules in the cell periphery. The amount of soluble cytosolic TPPP/p25 is low throughout interphase. At the beginning of mitosis before nuclear envelope breakdown, the green fusion protein starts to detach from the microtubules and at the end of prophase TPPP/p25 distributes homogenously (see Fig. S1 in supplementary material). In metaphase, TPPP/p25 accumulates slightly over the mitotic spindle, but most TPPP/p25 molecules are still not bound to microtubules. This slight accumulation of TPPP/p25 over the mitotic spindle is also visible in anaphase. The amount of free TPPP/p25 decreases only during cytokinesis when it associates with microtubules again and accumulates in higher amounts over the microtubule bundles crossing the cytokinetic cleavage furrow. The colocalization of TPPP/p25 with the microtubular structures in different stages of the cell cycle suggests that its major target is the microtubular filament system in mammalian cells in agreement with our previous in vitro data (Hlavanda et al., 2002; Tirian et al., 2003). Furthermore, the staining pattern suggests that TPPP/p25 binds stable interphase microtubules with high affinity, whereas its association with dynamic M-phase microtubules is less efficient. In order to follow TPPP/p25 distribution during the cell cycle in a more comparative way, we followed the fate of the fusion protein in a cell with very low levels of expression entering mitosis. Whereas a high proportion of TPPP/p25 still binds to microtubules four minutes before nuclear envelope breakdown (NEB), it starts to detach shortly before NEB, distributes nearly homogenously shortly after NEB, and accumulates slightly

over the mitotic spindle during metaphase (see Fig. S1 in supplementary material).

### FRAP analysis of microtubule-EGFP-TPPP/p25 interaction

The cell-cycle experiments described above indicated that the microtubule-bound fusion protein undergoes exchange with the surrounding cytoplasm. To gain information about the dynamics of TPPP/p25 association to the microtubular filaments, FRAP analysis was carried out with transfected NRK cells (Fig. 5A). The recovery rate suggests a very fast, dynamic interaction between the microtubular network and the EGFP construct: half of the bleached TPPP/p25 protein molecules were exchanged with labeled ones within 5 seconds even in the thick microtubule bundles (see Fig. 5D). The recovery rate was similar in the case of both the thin and the bundled type of filamentous structures. These observations are indicative of a fast dynamic association and exchange of TPPP/p25 to the highly organized structure of the interphase microtubules and bundles of microtubules of the NRK cells (Fig. 5).

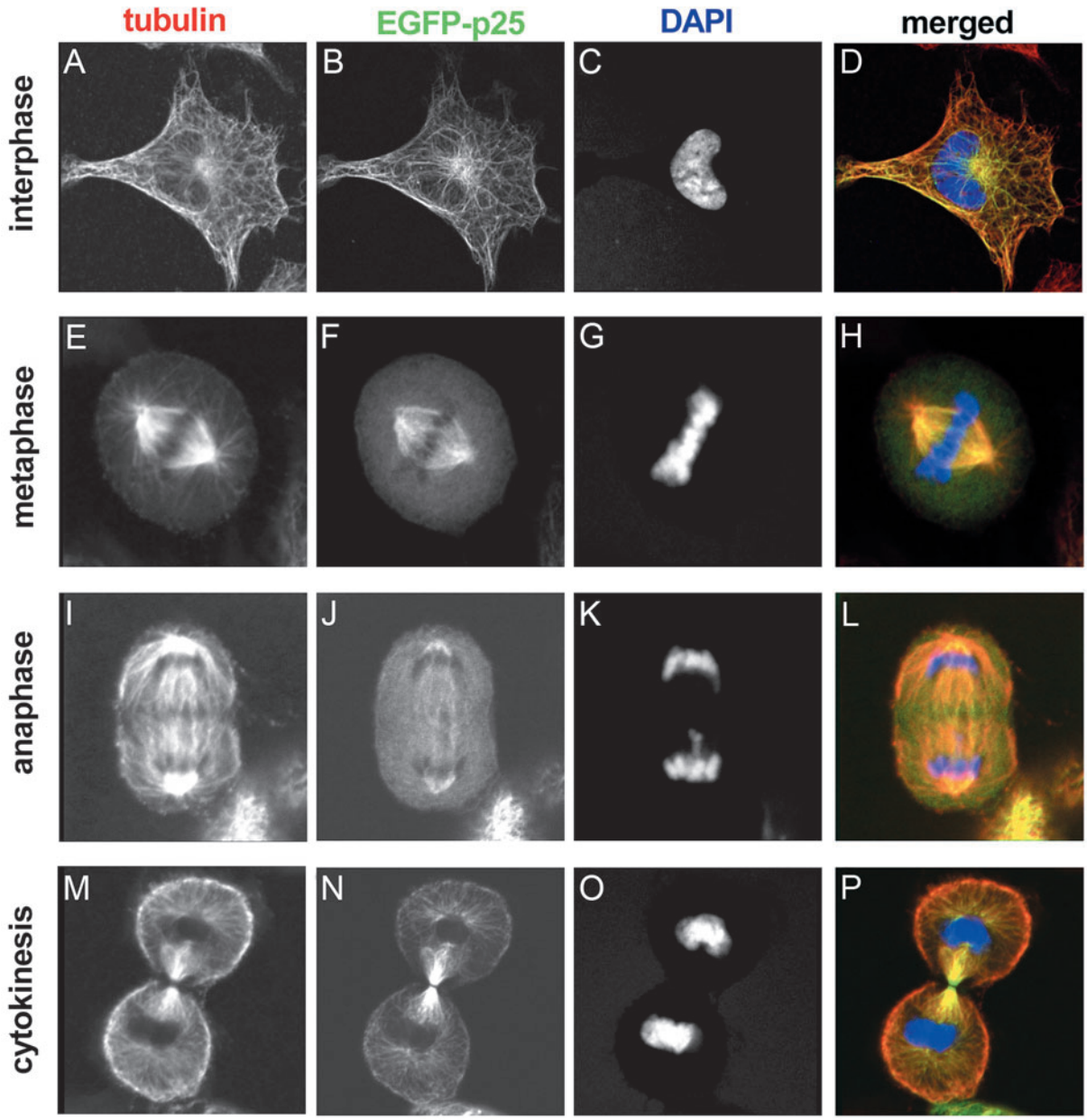


**Fig. 4.** EGFP-TPPP/p25 localization in transfected NRK cells at different stages of the cell cycle. Tubulin, TPPP/p25 and DNA are red, green and blue in the merged images, respectively. (A-D) At interphase TPPP/p25 localizes over the microtubules throughout the cell, but accumulates at a higher levels in the vicinity of the centrosome (green dominates in the merged image D). (F and J) From prophase (not shown) to late anaphase, free TPPP/p25 level is considerably higher in the cytoplasm. In metaphase (E-H) and anaphase (I-L) TPPP/p25 accumulation is detectable only over the spindle microtubules and the centrosomes. (M-P) The level of free TPPP/p25 decreases again at the telophase-cytokinesis transition and TPPP/p25 becomes preferentially enriched over the microtubules spanning the cytokinetic cleavage furrow.

### Formation of the aggresome and the perinuclear cage

As our recent data showed that the level of TPPP/p25 was elevated in human pathological brain tissues, specifically in those characteristic of α-synucleopathy, and that the protein accumulated in inclusion bodies (Kovacs et al., 2004), the intracellular ultrastructures induced by the extensive overexpression of EGFP-TPPP/p25 were studied in transfected HeLa cells. Two major types of structure could be identified by immunocytochemistry and electron microscopy: the aggresome and the perinuclear cage. The formation of these structures is not unique to HeLa cells; similar aberrant structures were seen in transfected NRK cells at high expression levels (data not shown). In most of the transfected HeLa cells in the high expression state, the nucleus became indented (Fig. 6A), frequently bi- or multilobed (Fig. 6B) and a large, strongly fluorescent juxtanuclear spot (aggresome) positioned in an indentation of the nucleus appeared in the cytoplasm. The microtubules were also strongly labeled, and sometimes formed disordered bundles. In

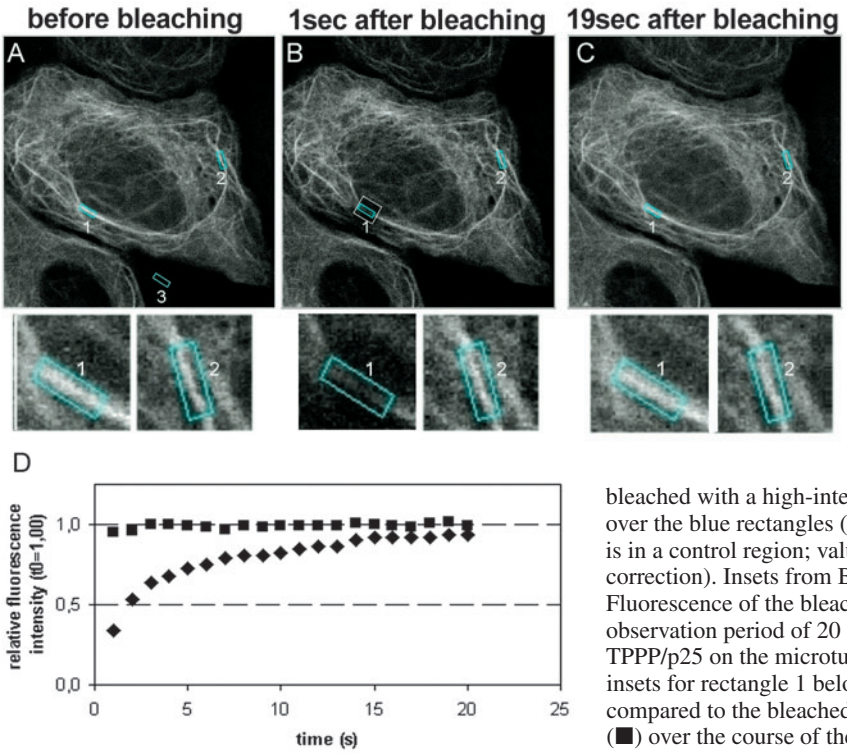


**Fig. 5.** Rapid exchange of EGFP-TPPP/p25 on microtubules demonstrated by FRAP. (A-C) NRK cells were transfected with pEGFP-TPPP/p25. The experimental region (white square shown in B) containing a thick microtubule bundle was bleached with a high-intensity laser beam. Fluorescent intensities were measured over the blue rectangles (rectangle 1 resides within the bleached area; rectangle 2 is in a control region; values from rectangle 3 were used for background correction). Insets from B and C are shown at 1 and 19 seconds, respectively. Fluorescence of the bleached region reappeared nearly completely during the observation period of 20 seconds indicating the very rapid exchange of TPPP/p25 on the microtubule bundle (compare the intensities of the enlarged insets for rectangle 1 below A and C). (D) The intensities of rectangle 1 compared to the bleached area (◆), and rectangle 2 compared to the control area (■) over the course of the experiment.

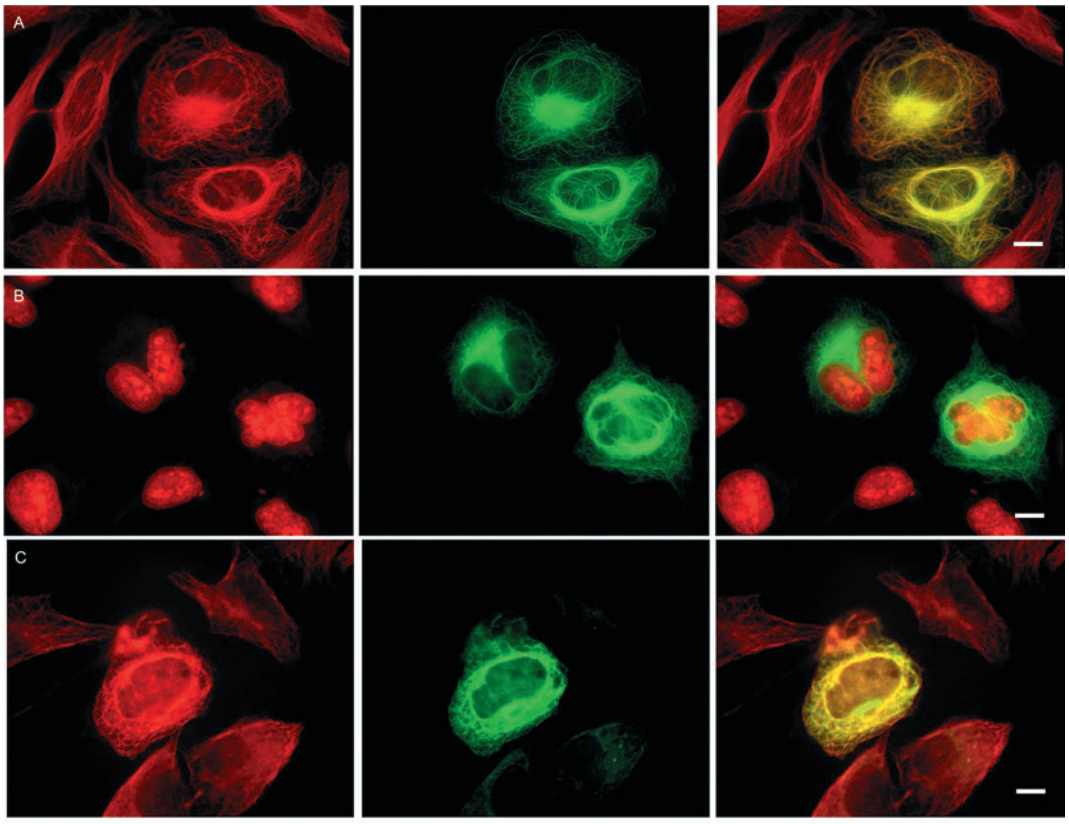


**Fig. 6.** Transfected HeLa cells in the high expression state. HeLa cells were transfected with pEGFP-TPPP/p25 (A and B) or pcDNA3-TPPP/p25 (C). After 20 hours, cells were fixed with ice-cold buffered ethanol. Tubulin was stained with anti-α-tubulin antibody (red) (A and C). (B) Nuclei were stained with ethidium bromide (red). Protein construct was detected as green EGFP signal in A and B. Expressed TPPP/p25 was detected by FITC-conjugated secondary antibody in C. Bars, 10 μm.

other cells, the microtubular network was totally rearranged and formed a prominent cage around the nucleus (perinuclear cage) (Fig. 6A). Similar or even more pronounced protein aggregation, aggresome formation, was observed in HeLa cells transfected with non-tagged TPPP/p25 detected by immunocytochemistry. Therefore, the formation of this characteristic structure was indeed induced by the presence of TPPP/p25 (Fig. 6C).

We characterized the structures formed in the presence of high levels of TPPP/p25 by examining the transfected cells by electron microscopy. One of the characteristic features of these cells is the clustering of cell components in the area of the centrosome identified by the presence of the centriole (data not shown). This process leaves the periphery of the cytoplasm free of mitochondria and cisternae of the rough endoplasmic reticulum (RER). In the center of the centrosomal area a distinct round body can frequently be observed that consists of a dense network of filamentous material composed of microtubules and 10 nm intermediate filaments. Inside its core the fibers run randomly, however in the periphery they tend to be arranged in parallel bundles. Within this network ribosomes and small cisternae of the RER and annulate lamellae are dispersed, however, mitochondria and Golgi membranes are excluded (Fig. 7). Another change observed in the cells highly expressing TPPP/p25 is the formation of the perinuclear cage. Ultrastructural examination reveals that the cage consists of bundles of densely packed, parallel-aligned microtubules and intermediate filaments running at different angles around the nucleus (Fig. 8).

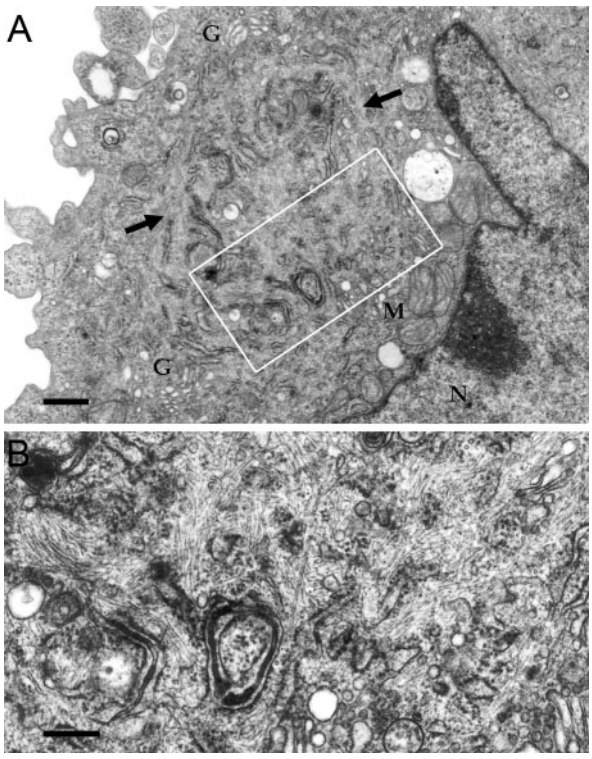


**Fig. 7.** Electron microscopy of the aggresome in a HeLa cell expressing TPPP/p25. (A) Aggresome-like body (marked by arrows) located in the cavity of a crescent-shaped nucleus. (B) High-power magnification of the area boxed in A showing the heavy accumulation of microtubules and intermediate filaments in this region. Golgi cisternae (G) and mitochondria (M) are located around the body. Bar, 600 nm (A); 300 nm (B). N, nucleus.

### Effect of proteosome inhibition on EGFP-TPPP/p25 expression

To elucidate the fate of the expressed chimeric protein, the ubiquitin-proteosome system was inhibited with MG132 (Carbobenzoxy-Leu-Leu-Leu-al) in transfected cells (Palombella et al., 1994; Lee and Goldberg, 1998). Parallel cultures of HeLa cells were transfected with pEGFP-TPPP/p25 plasmid and were incubated for 18 hours. Inhibitor was then added to the half of the cultures and all the samples were cultured for a further 2 hours. Next, samples were fixed and the transfected cells were counted. The average fluorescence of a cell was also calculated. According to our quantitative measures, the overall fluorescence of the microscopic field was increased about twofold in the presence of the inhibitor. The value of maximal intensity per pixel detected was similar in both types of sample (152 arbitrary units) at the same exposure. The average cell fluorescence was significantly higher in the presence of MG132 compared to untreated cells (Fig. 9). The increase in the number of fluorescent cells in the presence of MG132 was apparent as more fluorescent cells became visible because of less degradation of the fusion protein. In fact, at higher magnification, more aggresomes containing fluorescent cells were visualized in the presence of MG132 (data not shown). These data suggest that the TPPP/p25 level is controlled by the proteosome machinery and also that transiently expressed EGFP-TPPP/p25 is quickly degraded in HeLa cells.

### Effect of TPPP/p25 expression on the stability of microtubular networks

Our recent in vitro experiments have shown that isolated TPPP/p25 was bound to microtubules and induced bundling of the taxol-stabilized microtubules (Hlavanda et al., 2002). The effect of EGFP-TPPP/p25 on the stability of the microtubular network was investigated in transfected HeLa cells. Cells were treated with vinblastin, a specific microtubule-destabilizing agent. In untransfected cells, the microtubular network collapsed completely, leading to uniform distribution of tubulin signal in the cytosol (Fig. 10A). In transfected cells however, although some of the green fluorescence can be seen in the cytosol, microtubules were maintained as indicated by the alignment of EGFP-TPPP/p25 with bundled microtubules around the nucleus. These data show that the presence of TPPP/p25 counteracts the effect of vinblastin.

The stabilization of microtubule structures by TPPP/p25 is also supported by in vitro experiments using purified proteins. TPPP/p25 was incubated with taxol-stabilized microtubules at 37°C, which bundles the tubules. The bundling of microtubules caused an increase in the turbidity of the TPPP/p25-containing samples as we demonstrated by sedimentation experiments as well as by electron microscopy (Hlavanda et al., 2002). Therefore, the decrease in turbidity by destabilizing agents/conditions indicates the disassembly of both single and bundled microtubules. The depolymerization of the control and TPPP/p25-treated microtubules was induced by lowering the temperature from 37°C to 4°C in the absence and presence of

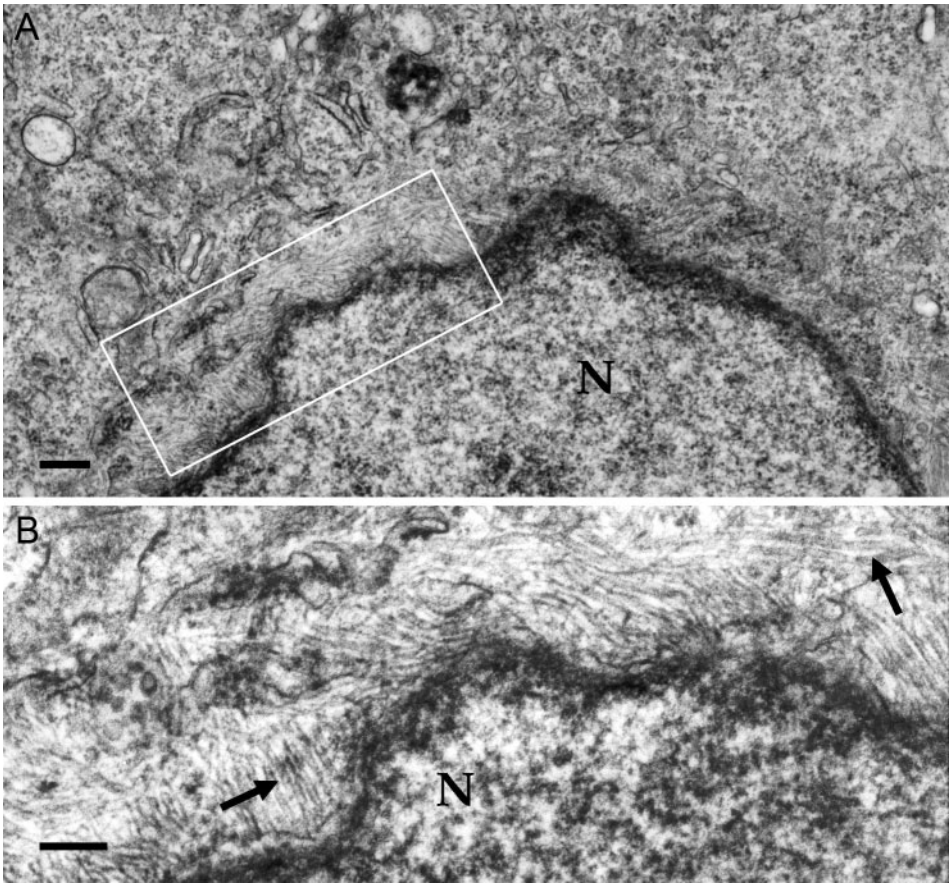


**Fig. 8.** Electron microscopy of the perinuclear cage in a HeLa cell expressing TPPP/p25. (A) Low power view of the perinuclear cage. (B) Enlarged view of the area framed in A showing that the cage consists of microtubules (arrows) organized into roughly parallel bundles running at different angles in close proximity to the nuclear membrane. N, nucleus. Bar, 300 nm (A); 150 nm (B).

$Ca^{2+}$ or vinblastin. Under these conditions, the TPPP/p25-treated samples display higher resistance to depolymerization as judged by turbidimetric measurements (Fig. 10B-D). Therefore, TPPP/p25 appears to be a protein that can stabilize the microtubular filaments/bundles.

## Discussion

In a recent work we showed that a new brain-specific protein, denoted TPPP/p25 can induce aberrant microtubule assemblies and ultrastructures even at substoichiometric concentrations and these structures were characterized by electron and atomic force microscopy (Hlavanda et al., 2002; Tirian et al., 2003). The effect of this protein on the mitotic process was investigated by injecting isolated protein into *Drosophila* embryos. Our data showed that mitosis was arrested as the TPPP/p25 diffused inside the large embryo and caused significant enlargement of the nuclei with normally segregated centrosomes (Tirián et al., 2003). Our present data provide evidence that the microtubular network is also the major target of TPPP/p25 in mammalian cells. HeLa and NRK cells do not have detectable levels of endogenous TPPP/p25, however, transfection using the pEGFP-TPPP/p25 plasmid construct rendered it possible to study the intracellular localization and its effect on the viability, morphology and the cytoskeletal architecture of mammalian cells as well as on some basic cellular functions during the expression of the fusion protein.

We observed that the number of fluorescent cells increased with time following transfection until about 20 hours. Some of these cells contained relatively low amounts of EGFP-TPPP/p25; the architecture of the cytoskeletal network and the hyperpolarization state of the mitochondrial membranes in these cells were similar to that of control cells (cf. Fig. 2A and B). Under these conditions the green fusion protein specifically aligned along the microtubular filaments by binding directly or indirectly to microtubules. According to our previous in vitro data, TPPP/p25 binds with high affinity ($K_d$=0.2 μM) to tubulin and microtubules (Tirian et al., 2003), thus our results obtained with transfected cells suggest that this interaction exists in living cells as well. Two lines of evidence demonstrate the dynamic nature of this interaction. First, we observed a very rapid recovery rate in FRAP experiments with live NRK cells (Fig. 5). Second, we found that the fusion protein changes its localization during phases of mitosis: it dissociates from spindle microtubules at the prophase and reassociates at later phases. The dynamic character of TPPP/p25 interaction with the microtubular system suggests that it is likely to be involved in the reorganization of microtubule ultrastructures (Fig. 4).

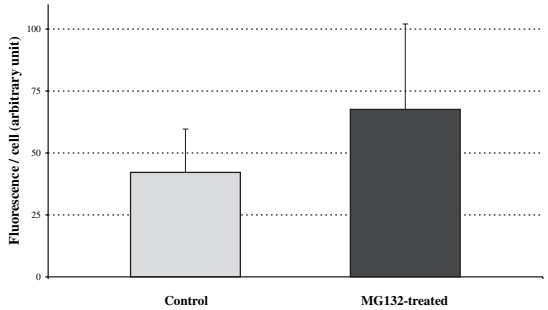


**Fig. 9.** Quantitative analysis of fluorescence intensity of transfected HeLa cells. Digital images were acquired through a 10× objective and analyzed with ImageJ software. Individual cells were identified and measured manually. The overall fluorescence of a cell was determined as the product of the measured area and average fluorescence intensity of the measured area (with average of background subtracted). Statistical comparison was done using the Student's *t*-test. The number of detected (transfected) cells within a microscopic field was 40±6 and 65±7 for the control and MG132-treated samples, respectively ($P \leqslant 0.001$).

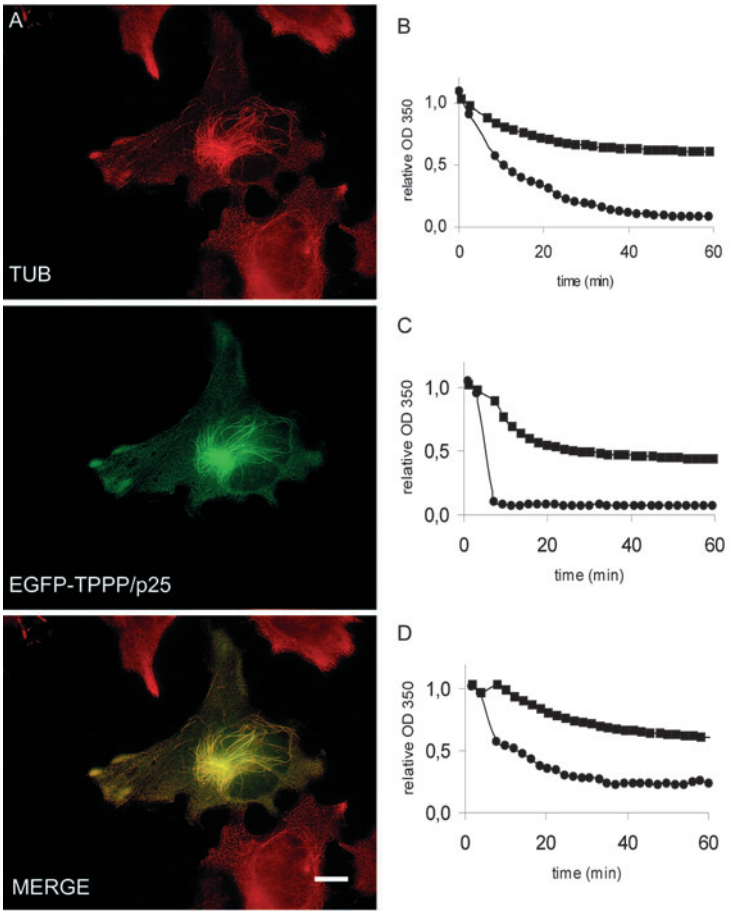


**Fig. 10.** Stability of TPPP/p25 bundled microtubules. (A) For the in vivo assay, transfected cells were treated with 100 nM vinblastin in the final 2 hours of the incubation period. Tubulin was detected by immunocytochemistry (red). Green signal originated from EGFP-TPPP/p25. In the presence of vinblastin, in non-transfected cells (red only), the microtubular network is completely dissolved. Fine fibers in the cytoplasm are not detected after vinblastin treatment, but bundled, tubulin-positive fibers were preserved. Note the colocalization pattern of red and green signal in merged image in A. (B-D) Effect of low temperature (4°C; B), plus 0.75 mM $Ca^{2+}$ (C) or plus 5 μM vinblastin (D) on the taxol-stabilized microtubules treated (■) and untreated (●) with TPPP/p25. 15 μM tubulin was polymerized by addition of 20 μM taxol with and without 3 μM TPPP/p25 at 37°C for 15 minutes in PEM buffer. $Ca^{2+}$ and vinblastin were added and the depolymerization of microtubules was followed by turbidimetry for 60 minutes at 4°C. Bar, 10 μm.

The role of p25α (which corresponds to TPPP/p25) in the synaptic structural reorganization by interacting with the structural protein, complexin has been recently proposed (Nelson et al., 2004).

The number of heavily transfected cells significantly increased as the expression of EGFP-TPPP/p25 proceeded. After 20-30 hours, mitosis was arrested in the highly fluorescent cells, which was followed by cell death (c.f. Figs 1, 2 and 6). Treatment of these cells with the proteosome inhibitor, MG132, enhanced the relative occurrence of bright fluorescent cells (Fig. 9). This indicates the active involvement of the proteosome machinery in the degradation of excess unfolded protein.

Formation of pericentriolar membrane-free, cytoplasmic inclusions containing filamentous proteins was first described in cells expressing misfolded membrane CFTR (cystic fibrosis transmembrane conductance regulator) protein (Johnston et al., 1998). This inclusion body-like protein aggregate, which was formed in the presence of proteosome inhibition, was denoted the aggresome.

Based on the intracellular and ultrastructural features of the bright fluorescent aggregate, we identified the round juxtanuclear bodies as aggresomes. The mechanism leading to the formation of such aggregates is unclear, yet in the case of TPPP/p25, the active involvement of the microtubular system for the formation of such structures seems to be crucial as suggested by Kopito (Kopito, 2000). At the ultrastructural level, the large round juxtanuclear structure contains a dense network of microtubules and intermediate filaments interdispersed with small cisternae of RER. Membranes of the RER form closely apposed pairs between which dense material is deposited (Figs 7 and 8). At the electron microscopic level TPPP/p25 produced quite distinct ultrastructures when compared to those defined by Kopito (Kopito, 2000). For example, we did not observe the accumulation of dense particles 50-90 nm in size inside the EGFP-TPPP/p25-induced aggresomes, analogous to the particles reported by others (Johnston et al., 1998; Garcia-Mata et al., 1999).

Interestingly, the extensive expression of EGFP-TPPP/p25 in mammalian cells always resulted in another distinct cell type: the perinuclear cage, which consisted of heavily bundled microtubules and intermediate filaments. In these aberrant cells mitochondria do not take up TMRE, indicating the collapse of the mitochondrial membrane potential and as a consequence, the failure of energy supply in these cells. Previously we showed that TPPP/p25 bundles taxol-stabilized microtubules in vitro (Hlavanda et al., 2002); here we provided evidence that this protein may also act as a bundling agent in living cells. Indeed, these ultrastructural alterations may confer the high stability of these microtubules against depolymerization effects (Fig. 10) despite the dynamic heteroassociation of TPPP/p25 with structural proteins, and may result in mitotic arrest as detected in *Drosophila* embryos injected with isolated TPPP/p25 (Tirian et al., 2003).

Before we discovered TPPP/p25 as a tubulin polymerization-promoting protein there was very little data concerning its occurrence and virtually nothing on the role of its appearance in inclusions of pathological brain tissues. Recently we reported that in non-diseased human brains TPPP/p25 immunopositivity is present in glial cells mainly in the white matter, in addition to perineuronal glial cells in the cortex and faint immunostaining in the neuropil (Kovacs et al., 2004). TPPP/p25 was only slightly expressed during the embryonic period in rat brain, and the expression increased extensively in the first weeks after birth then gradually increased until 1-2 years of age (Takahashi et al., 1993). In human pathological brain tissue the extensive accumulation of TPPP/p25 was detected in Lewy bodies and glial inclusions. This suggests that TPPP/p25 might be a molecular player in events leading to cell death in these disorders. Inclusion body formation in some neurodegenerative disorders has been proposed to be an aggresome-related

response to abnormal protein (McNaught et al., 2002). Indeed, a close relationship between Lewy bodies and aggresomes, formed at the centrosome to sequester and degrade excess levels of potentially toxic abnormal protein has been suggested by the finding that centrosome/aggresome-related proteins, γ-tubulin and pericentrin display an aggresome-like distribution in Lewy bodies containing α-synuclein, ubiquitin and neurofilaments. The overexpression of TPPP/p25 in mammalian cells may mimic these processes, and the characteristic Lewy body proteins were colocalized with TPPP/p25 in PD and DLB (Kovacs et al., 2004). We propose here that the formation of inclusion body-like structures during the expression of this unfolded brain-specific protein might be related to the slow pathological processes that finally lead to neurodegenerative disease. One can hypothesize that the unbalanced homeostasis of neurons or glial cells leads to an overload of structural proteins like TPPP/p25 in a similar manner to tau isoforms or α-synuclein.

Although the cause of the rearrangements of the cytoskeleton and formation of aberrant intracellular structures by TPPP/p25 accumulation, and their relation to cell death remains unclear, the long-term accumulation of proteinaceous aggregates near the centrosomes could interfere with intracellular transport and alter other cytoskeletal functions. This could explain the death of the transfected cells and may contribute to the understanding of the pathology and development of neurological diseases.

We are grateful to Prof. P. H. Jensen of the University of Aarhus for providing the TPPP/p25 plasmid, and to Prof. Tamás Vicsek for providing the conditions for time-lapse microscopy and Dávid Selmeczi for his help in processing our time-lapse data. This work was supported by the Hungarian National Scientific Research Fund Grants OTKA T-046071 and B-044730; Hungarian Ministry of Education Grant OMFB-00701/2003 and Charles Simonyi fellowship (to J.O.), Hungarian Ministry of Education Grant OMFB 00703/2003 (to J.K.) and Bolyai fellowship (to L.T.), OTKA T034995 and NKFP 3A/0005/2002 (to B.Sz.).

## References

**Beaudouin, J., Gerlich, D., Daigle, N., Eils, R. and Ellenberg, J.** (2002). Nuclear envelope breakdown proceeds by microtubule-induced tearing of the lamina. *Cell* **108**, 83-96.

**Collins, T. J. and Bootman, M. D.** (2003). Mitochondria are morphologically heterogeneous within cells. *J. Exp. Biol.* **206**, 1993-2000.

**Daigle, N., Beaudouin, J., Hartnell, L., Imreh, G., Hallberg, E., Lippincott-Schwartz, J. and Ellenberg, J.** (2001). Nuclear pore complexes form immobile networks and have a very low turnover in live mammalian cells. *J. Cell Biol.* **154**, 71-84.

**Garcia-Mata, R., Bebok, Z., Sorscher, E. J. and Sztul, E. S.** (1999). Characterization and dynamics of aggresome formation by a cytosolic GFP-chimera. *J. Cell Biol.* **146**, 1239-1254.

**Goedert, M.** (2001). The significance of tau and alpha-synuclein inclusions in neurodegenerative diseases. *Curr. Opin. Genet. Dev.* **11**, 343-351.

**Hegedus, B., Czirok, A., Fazekas, I., Babel, T., Madarasz, E. and Vicsek, T.** (2000). Locomotion and proliferation of glioblastoma cells in vitro: statistical evaluation of videomicroscopic observations. *J. Neurosurg.* **92**, 428-434.

**Hlavanda, E., Kovacs, J., Olah, J., Orosz, F., Medzihradszky, K. F. and Ovadi, J.** (2002). Brain-specific p25 protein binds to tubulin and microtubules and induces aberrant microtubule assemblies at substoichiometric concentrations. *Biochemistry* **41**, 8657-8664.

**Iijima, T., Mishima, T., Tohyama, M., Akagawa, K. and Iwao, Y.** (2003). Mitochondrial membrane potential and intracellular ATP content after transient experimental ischemia in the cultured hippocampal neuron. *Neurochem. Int.* **43**, 263-269.

**Johnston, J. A., Ward, C. L. and Kopito, R. R.** (1998). Aggresomes: a cellular response to misfolded proteins. *J. Cell Biol.* **143**, 1883-1898.

**Junn, E., Lee, S. S., Suhr, U. T. and Mouradian, M. M.** (2002). Parkin accumulation in aggresomes due to proteasome impairment. *J. Biol. Chem.* **277**, 47870-47877.

**Kopito, R. R.** (2000). Aggresomes, inclusion bodies and protein aggregation. *Trends Cell Biol.* **10**, 524-530.

**Kovacs, G. G., Laszlo, L., Kovacs, J., Jensen, P. H., Lindersson, E., Botond, G., Molnar, T., Perczel, A., Hudecz, F., Mez, G. et al.** (2004). Natively unfolded tubulin polymerization promoting protein TPPP/p25 is a common marker of alpha-synucleinopathies. *Neurobiol. Dis.* **17**, 155-162.

**Lee, D. H. and Goldberg, A. L.** (1998). Proteasome inhibitors: valuable new tools for cell biologists. *Trends Cell Biol.* **8**, 397-403.

**Martin, C. P., Vazquez, J., Avila, J. and Moreno, F. J.** (2002). P24, a glycogen synthase kinase 3 (GSK 3) inhibitor. *Biochim. Biophys. Acta* **1586**, 113-122.

**McNaught, K. S., Shashidharan, P., Perl, D. P., Jenner, P. and Olanow, C. W.** (2002). Aggresome-related biogenesis of Lewy bodies. *Eur. J. Neurosci.* **16**, 2136-2148.

**Nelson, T. J., Backlund, P. S., Jr and Alkon, D. L.** (2004). Hippocampal protein-protein interactions in spatial memory. *Hippocampus* **14**, 46-57.

**Palombella, V. J., Rando, O. J., Goldberg, A. L. and Maniatis, T.** (1994). The ubiquitin-proteasome pathway is required for processing the NF-kappa B1 precursor protein and the activation of NF-kappa B. *Cell* **78**, 773-785.

**Takahashi, M., Tomizawa, K., Fujita, S. C., Sato, K., Uchida, T. and Imahori, K.** (1993). A brain-specific protein p25 is localized and associated with oligodendrocytes, neuropil, and fiber-like structures of the CA3 hippocampal region in the rat brain. *J. Neurochem.* **60**, 228-235.

**Tanaka, M., Kim, Y. M., Lee, G., Junn, E., Iwatsubo, T. and Mouradian, M. M.** (2004). Aggresomes formed by alpha-synuclein and synphilin-1 are cytoprotective. *J. Biol. Chem.* **279**, 4625-4631.

**Tirian, L., Hlavanda, E., Olah, J., Horvath, I., Orosz, F., Szabo, B., Kovacs, J., Szabad, J. and Ovadi, J.** (2003). TPPP/p25 promotes tubulin assemblies and blocks mitotic spindle formation. *Proc. Natl. Acad. Sci. USA* **100**, 13976-13981.

**Uversky, V. N.** (2002a). What does it mean to be natively unfolded? *Eur. J. Biochem.* **269**, 2-12.

**Uversky, V. N.** (2002b). Natively unfolded proteins: a point where biology waits for physics. *Protein Sci.* **11**, 739-756.